Environmental Pollution 345 (2024) 123500

Contents lists available at ScienceDirect

Environmental Pollution

journal homepage: www.elsevier.com/locate/envpol

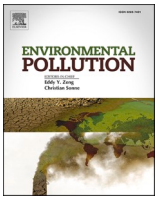

Trace metal partitioning in the parnaíba delta in dry season, equatorial coast of Brazil☆

Thays Thayanne Luz Santos [a,b,*], Jean Louis Stéphane Mounier [b], Rozane Valente Marins [a]

[a] Federal University of Ceará, Marine Science Institute/LABOMAR, Av. da Abolição, 3207, 60.165-081, Fortaleza, CE, Brazil
[b] Université de Toulon, Aix Marseille Univ., CNRS/INSU, IRD, MIO UM 110, Mediterranean Institute of Oceanography, CS, 60584, 83041, Toulon, France

ARTICLE INFO

Handling editor: Hefa Cheng

Keywords:
Estuaries
Metallic contamination
Distribution coefficient
Dry season

ABSTRACT

Trace metal concentrations in the particulate fractions (MP), dissolved fractions (MD) and sediments (MS), such as Ba, Cu, Co, Cr, Pb, Ni and Zn, were determined during the dry season of the largest open sea delta of Americas, the Parnaíba River Delta (Brazil). This study aimed to comprehend the distribution, dynamic changes of metal speciation and environmental quality index of trace metals in the particulate fractions and subsurface sediments in scenario of major marine influence over the delta. The trace metals bound to suspended particulate material (SPM) from weathering the drainage basin exhibited a removal trend under increases in salinity and pH. Desorption influenced the partitioning of Ba_{MP}, Zn_{MP}, Ni_{MP}, Co_{MP}, Cu_{MP}, and the adsorption and precipitation of Pb_{MP} and Cr_{MP} to the surface sediments. The organic matter contents in the sediments acts as an important geochemical carrier of these contaminants, and the dissolved organic carbon influences the binding of Pb_{MD} in the subsurface waters. The geoaccumulation index (Igeo) plays a crucial role in revealing potential contamination with Zn_{MP} contents and weak association to this fraction. These results make possible the assessment of ecological risk by metal contamination and global pollution mitigation in coastal tidal estuaries under intensive physical mixing along the equatorial coast.

1. Introduction

The Parnaíba River Delta (PRD) is the largest open sea delta in the Americas, and the third in the world, after the Nile delta in Africa and the Mekong delta in Asia (Guimarães-Costa et al., 2019). It is also placed in the third largest mangrove forest in the world, with 7 % of the global mangrove area, which are known to be important drivers of the coastal organic and inorganic element budgets, acting usually as a sink of trace metals due to their richness in organic matter (Diniz et al., 2019; FAO, 2020; Mori et al., 2019; Thanh-nho et al., 2018).

Besides being conserved as a primitive ecosystem, the PRD shows some evidence of urban and industrial contributions, with point sources of nutrients and trace metals entering the estuary (Paula Filho et al., 2021). Coastal environments are important for biological diversity because they provide many different habitats for breeding places and nurseries for various estuarine and marine species, and these regions are under the impact of sea level increase. In tropical areas, water retention in dams and decreased rainfall, due to El Niño events, intensifies this impact and alter the lability of trace metals (Lacerda et al., 2020). Therefore, studies about transport and availability of suspended trace metals give a piece important information about a possible risk of pollution in estuarine environments and their biodiversity during a dry season scenario when marine intrusion has the potential to simulate higher sea level conditions.

Trace metals evaluation in the PRD determined regional background levels (geochemical baseline) in sediments for Zn, Cu, Pb, Cr, Mn, and Fe (Paula Filho et al., 2015). However, continuous studies in this extensive area of 3132 km^2 pointed to values higher than the background for Cu, Ni, Zn and Fe (Paula Filho et al., 2019; 2021). The active and seasonal PRD hydrodynamics, with the presence of bays, large creeks, and anthropogenic and natural contributors to the region, besides the fate of a wave/tide dominated delta, probably induce variations along recent years.

The variation of physicochemical parameters along estuaries (such as salinity, pH, turbidity, dissolved oxygen, redox potential) affects the adsorption and desorption of trace metals, causing the mobilization to the dissolved phases and the solid phases (particulate fractions and sediments) that potentially modify the bioavailability of the metals

☆ This paper has been recommended for acceptance by Hefa Cheng.

* Corresponding author. Federal University of Ceará, Marine Science Institute/LABOMAR, Av. da Abolição, 3207, 60.165-081, Fortaleza, CE, Brazil.
E-mail addresses: thays_luzsantos@hotmail.com (T.T.L. Santos), stephane.mounier@univ-tln.fr (J.L.S. Mounier), rmarins@ufc.br (R.V. Marins).

https://doi.org/10.1016/j.envpol.2024.123500
Received 18 August 2023; Received in revised form 14 January 2024; Accepted 3 February 2024
Available online 4 February 2024

(Bianchi, 2007; Gaulier et al., 2021; Wang and Wang, 2016). Therefore, to improve the knowledge on the behavior of the trace metals in PRD, it is important to determinate the partitioning of trace metals to comprehend their degree of mobility and availability in aquatic environments (Guillén et al., 2012; Yao et al., 2016) in a diverse estuarine environment with a major river, mangrove channels and bays that can reflect the influence of saline intrusion in times of climate changes. Lacerda et al. (2020) identify a phenomenon known as the Arctic Paradox, that is the reduction of continental runoff that increase the residence time and accumulation of particulate organic-Hg complexes in the estuary. The Hg will enter food webs, increasing contamination of the biota and human exposure.

Thereby, the distribution coefficients (Kd) of trace metals between solid (particulate fractions and sediments) and dissolved fractions can enrich the knowledge on trace metal fate in the PRD compartments to assess the future environmental risks, particularly in a global scenario of sea level increase (Lindsey, 2021). Additionally, it suppress the lack of data on trace metal in subsurface waters in the Brazilian equatorial coast (Marengo et al., 2017; Santos et al., 2023), a region between Amazonian tropical climate and Northeastern semiarid areas (Veiga Júnior, 2000). The present study aims to comprehend the distribution, dynamic changes of metal partitioning, and geochemistry of seven metals (Ba, Cu, Co, Cr, Pb, Ni and Zn) in the environmental compartments of PRD.

2. Materials and methods

2.1. Environmental setting and sampling

Parnaíba River Delta (PRD) is located in the Equatorial Zone of Northeast Brazil at the geographic coordinates on the longitude 41°49′10″ W and latitude 2°50′15″ S. Due to its socio-environmental importance, it is inserted into an Environmental Protection Area (APA), with an area of 313.000 ha including 10 cities over Maranhão, Piauí and Ceará states (Guzzi, 2012; IBGE, 2020; Magalhães et al., 2008). It encompasses 85 islands along an area of 3132 km^2, including a complex mosaic of ecosystems, where the east side of the delta is placed the Parnaíba River with very low declivity (up to 50 cm km^{-1}), and in direction to the west side are situated large bays with intense mangrove channels, salt marshes and sandy beaches (Aquino da Silva et al., 2019; Guzzi, 2012).

The vegetation of PRD is represented by a dry coastal ecosystem, dunes, paleo dunes, and mangroves swamp forest flooded by seawater mixed with freshwater from rivers and streams. The main mangrove plant genera in the region are *Rhizophora*, *Laguncularia* and *Avicennia* that can reach 40 m in height (Guzzi, 2012). The hydrodynamic is characterized by meso-tidal with amplitudes ranging from 0.2 to 4.0 m under semidiurnal regime (CHN, 2019). The western part of the delta is dominated by waves and tides with two active channels and large mangrove creeks (Aquino da Silva et al., 2019). Some of these channels are large creeks where cargo and tourist boats sail.

The Intertropical Convergence Zone (ITCZ), which is the main system associated with precipitation distribution, is characterized by two established seasons: rainy season from January to June, with maximum monthly precipitation of 268 mm; and the dry season during July to December, with monthly maximum precipitation of 38.5 mm (INMET, 2020).

The geology of the PRD is characterized by the Cenozoic sedimentary sequence of small thickness, almost entirely composed by clayey and sandy sediments of fluvial and fluvial-marine origin (Costa, 2019). The Parnaíba River passes through the Parnaíba and Barreirinhas sedimentary basins, transporting their sediments until the APA. The mineral assemblages are compose mainly of quartz and ilmenite, and the occurrence of cordierite, cummingtonite and garnet are abundant in the river and decreases in westward (Smith et al., 2021). The riverine sediment supply increases from 50 mg L^{-1} at the mouth of the Parnaíba River to 71 mg L^{-1} at a location approximately 8.1 km upstream. However, in the offshore direction, it is observed a decrease to 11 mg L^{-1} depicting a sharp interface between the high turbid river plume and low suspended particulate material (SPM) seawater (Aquino da Silva et al., 2019). However, with forecasts of sea level rise and the observation of erosion processes being intensified on the northeast equatorial coast, these values may be continually changing (Godoy and Lacerda, 2014; Muehe, 2010).

Subsurface water samples were taken below the surface with a 2 L Niskin water sampler, pre-cleaned with HNO_3 and washed with Milli-Q water. The campaign was performed in December 2019, distributed at 13 stations along the PRD, during 21 h under spring tide conditions. The stations were distributed along geographic zones of PRD: main river (P01, P02 and P03), mangrove channel (P04, P05 and P06), and bay area (P07 to P13) as observed in Fig. 1. The water samples were filtrated with cellulose nitrate filters of 0.45 μm and diameter 47 mm, pre-cleaned with HCl 10% and Milli-Q water, dried, and recorded weight. Filtered water samples were separated in pre-cleaned (HCl 10%) high-density polyethylene (HDPE) bottles of 250 mL. Drops of HCl (37%) were added to make a pH < 2 to determine the dissolved trace metal. Additionally, 250 μL of NaN_3 (1 mM final concentration) was added to determinate the dissolved organic carbon (DOC).

Surface sediments were performed with a carbon steel dredge distributed at 11 stations (no samples at stations P08 and P13). Samples were handled with plastic shovel and box, and stored in a and labeled plastic bag. The dissolved fraction, particulate fraction and sediment samples were stored at 4 °C in the dark before further processing. All the apparatus were pre-cleaned with 10% HCl and rinsed with Milli-Q water. The physicochemical parameters (temperature and salinity), and pH of the subsuperficial waters were measured *in situ* using a handheld multi-parameter probe (YSI Professional Plus) and pH-meter (Methrom® 826).

2.2. Analytical procedures

The cellulose nitrate filters with retained solids were dried at 60 °C in an oven and weighted to quantify the suspended particulate material (SPM). SPM (mg L^{-1}) was determined by the equation $[(W_2 - W_1) \times 1000]/V_f$, where W_1 (g) is the initial weight of dry filter, W_2 (g) is the final weight of dry filter after filtration, and V_f (L) is the filtered water. DOC concentrations were measured by the high-temperature combustion technique using the TOC-V_{CSH} analyzer (Shimadzu), with an accuracy of 0.1 mg C L^{-1}. Surface sediments were gone through the same drying process and passed in the nylon mesh sieve set of different sizes (2.00 mm–63 μm) to determinate the grain-size according to the classification of the Folk and Ward (1957). Percentage of total organic matter (OM) contents in the sediments was determined following the loss-on-ignition method of Nóbrega et al. (2015). It was used the fraction <2 mm to determinate the trace metal contents in the sediments. Filters and sediments were mineralized by Ultrawave Single Reaction Chamber Microwave Digestion System (Milestone Inc) with the addition of 10 mL of aqua regia (HCl: HNO_3, 3:1, Fisher Scientific Trace Analysis grade) in 50 mL Teflon (PTFE). Subsequently, the substrates were filtered by a pre-cleaned online filter (0.45 μm, Whatman) to determinate the trace metal concentrations. It was measured Ba, Cr, Co, Cu, Ni, Pb, and Zn in the dissolved fractions (MD), particulate fractions (MP) and sediments (MS) using the HR-ICP-MS instrument. Indium (In) was used as an internal standard for quality control. The calibration was carried out with appropriate dilutions of a multi-element stock solution. The coefficient of variation (CV) accepted was below 2% for all metals. The precision and accuracy of the metal's methodology in suspended matter and sediments was tested with certified sediment reference materials for river sediment (LGC6817 by LGC Standards Ltd) and marine sediment (PACS-2 by National Research Council of Canada). The recoveries of metals ranged from 72.5 to 112.7%. Ba and Co have no referenced values in certified marine sediment material.

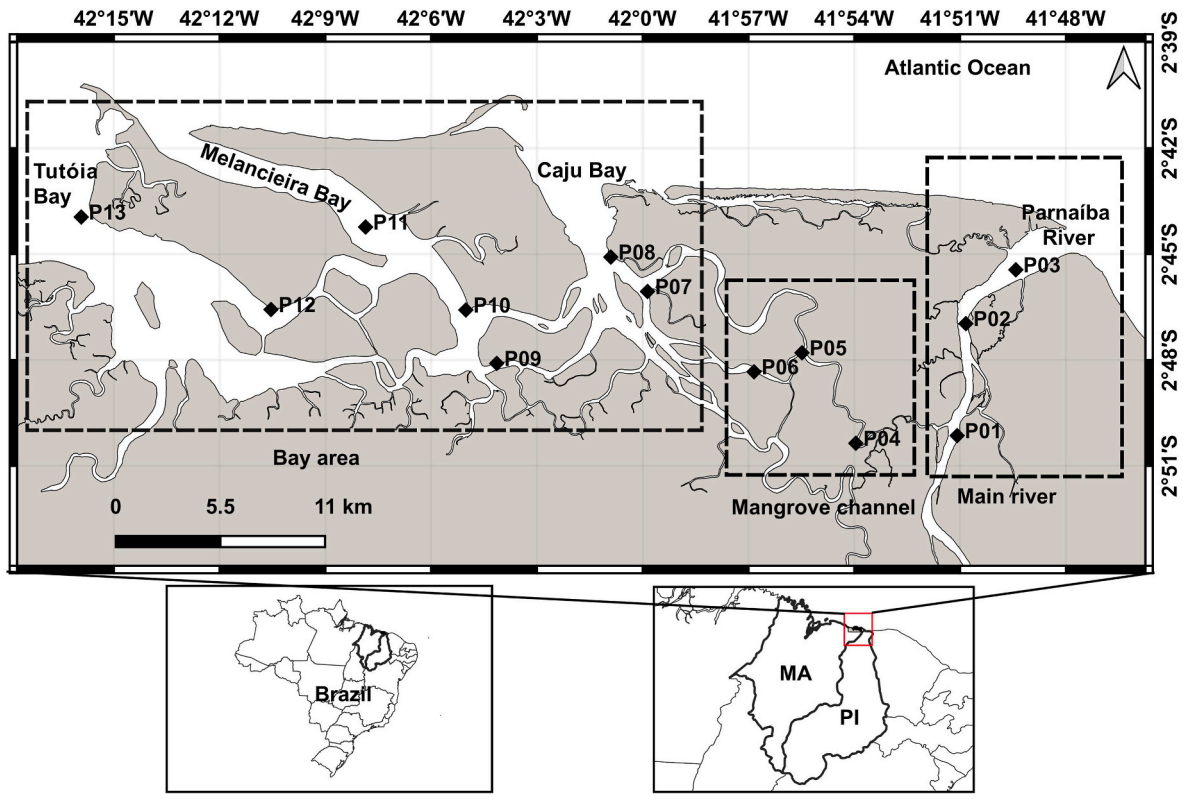

Fig. 1. Location map of sampling sites along the Parnaíba River Delta in the Equatorial Zone of Northeast Brazil.

2.3. Distribution coefficient (Log (Kd))

The distribution coefficient $(Log(Kd))$ is one of the most important parameters for assessing the migration potential of a contaminant present in the liquid phase that is in contact with sediments or SPM (Nabelkova and Kominkova, 2012). It was calculated using the logarithm of the ratio of trace metal concentrations between the solid phase, in the particulate fractions and sediments (μg kg^{-1}) and dissolved fractions (μg L^{-1}) as the follow equation $Log(Kd) = log[MP\ or\ MS\ /MD]$, where MP, MS and MD represents trace metals in particulate fractions, sediments and dissolved fractions, respectively. According to Nabelkova and Kominkova (2012), values of Log (Kd) ≤3 are present preferentially in the liquid phase, while values of Log (Kd) < 4 characterize chemicals more easily released from solid phases, and Log (Kd) ≥5 represents trace metals bind into solid phases and only marginally migrate into a liquid phase (Nabelkova and Kominkova, 2012; Thanh-nho et al., 2018). However, it is important to observe that the authors did not classify Log (Kd) values between 4 and 5. Therefore, in the present study, values ranging between 3< Log (Kd) < 5 will be characterized as elements more easily released from solid phases.

2.4. Geoaccumulation index (Igeo)

The concentration of trace metals is not enough to identify anthropogenic input of contaminants in the environment, as trace metals come from geological basement too. Therefore, it was necessary to determinate an index of sediments and particulate fractions quality. Geoaccumulation Index (Igeo) was applied using the formula $Igeo = log_2(Cn/1.5 \times Bn)$, where Cn (μg g^{-1}) is the concentration of trace metals in the particulate fractions and sediments, Bn (μg g^{-1}) is the geochemical background value, and the constant 1.5 is the correction factor for the possible lithological variability of the sediments (Marins et al., 2004; Müller, 1986). Igeo is classified in seven classes, where Class 0 is uncontaminated (Igeo≤0) and Class 6 is extremely contaminated (Igeo≥5). For the metals analyzed in the present study, there is the only one study reporting on regional background for Cu (6.8 μg g^{-1}), Cr (18.0 μg g^{-1}), Pb (5.9 μg g^{-1}) and Zn (13.4 μg g^{-1}) in the literature to PRD (Paula Filho et al., 2015).

2.5. Statistical analysis

The Shapiro-Wilk test was used to assess the normality of physical and chemical variables in the waters of PRD. When it exhibited normal distribution (parametric), homoscedasticity of variance (Bartlett's test), and one-way analysis (ANOVA) were used to determine the significant differences between the zones (main river, mangrove channel, and bay area). Although, when the data were not normally distributed, Levene's test and Kruskal-Wallis were applied. Spearman's rank correlation method (correlation coefficient r) was applied to observe possible correlations among variables. Wilcoxon rank-sum tests were applied to observed differences between the mean of Igeo and Log (Kd) between the compartments. All tests consider the level of significance $\alpha = 0.05$. A principal component analysis (PCA) was applied to investigate the distribution of trace metals with the physicochemical in the environmental compartments of PRD. All statistical analyses were performed using the software RStudio 2022.12.0 + 353 "Elsbeth Geranium".

3. Results

3.1. Hydrodynamic condition and physicochemical parameters

The temperature showed no significant differences among the zones ($p > 0.05$, $n = 13$), exhibiting the range 29.0–29.9 °C (29.4 ± 0.2 °C). The DOC also exhibited no significant difference ($p > 0.05$, $n = 13$). However, it is noticeable that the one-way ANOVA may not have been sensitive enough to detect the spatial variation for DOC inside of each zone, which had different sample numbers, as observed in the main river and bay area described further (Table S1, Supplementary Material). The

salinity, pH and SPM exhibited a significant difference among the zones ($p < 0.05$, $n = 13$). This spatial variation collaborates with a previous study that identified different zones according to spatial fluctuations of the physicochemical parameters (Chielle et al., 2023).

The tide showed a minimum and maximum height of 0.1–3.2 m during the collecting campaign. The main river channel exhibited a typical longitudinal salinity and pH gradient during the dry season under the flood tide. This gradient resulted from the mixing of freshwater with seawater in the main river, with salinity values varying from 0.0 to 36.2 g kg^{-1} and pH values from 7.41 to 8.10. Additionally, DOC concentrations increased seaward with values from 7.0 to 17 mg L^{-1}, while the SPM decreased from 28.4 to 21.1 mg L^{-1}. The rise of the DOC may be related to the desorption from the particulate organic matter during the flood tide in the main river (García-Martín et al., 2021).

The sampling in the mangrove channel occurred in the sequence of stations P04 and P05 under the ebb tide, and P06 in the beginning of the flood tide. It was observed that there was an increase in pH from acidic (6.78) to slightly alkaline (7.18), and a rise in salinity from a low value of 2.3 g kg^{-1} to an intermediary value of 15.3 g kg^{-1}. The DOC in this zone decreased from 10.7 to 5.9 mg L^{-1}, with the changing tide. While the SPM increased from 18.2 to 47.7 mg L^{-1} with the rise in salinity, it probably showed that tide forces cause erosion on the margins and bottom of the channel, suspending the material deposited in the sediments to the waters of PRD.

Bay area sampling happened during the flood tide over stations P07, P08, P09 and P10, changed to the ebb tide in stations P11, P12, and P13. Despite the variation in tidal conditions, all these stations exhibited salinity values above 33.3 g kg^{-1} (35.2 ± 1.1 g kg^{-1}), and pH ranged from slightly alkaline (7.7) to more alkaline (8.1). The spatial distribution of DOC and SPM did not exhibit a clear variation along the bay area. However, both parameters showed the highest values under the ebb tide with 13.3 mg L^{-1} for DOC in the station P13, and 156.2 mg L^{-1} for SPM in station P12, both in the Tutóia Bay.

These results indicate that the PRD exhibits varying hydrodynamic conditions across different zones, which are strongly influenced by the saline intrusion, and consequently by the tides.

3.2. Trace metal in the particulate fractions

The trace metals in the particulate fractions demonstrated a removal trend with an increase in salinity in the main river and mangrove channel. These zones exhibited a remarkable decrease for Ba_{MP}, Co_{MP} and Pb_{MP} between three and four times, except to Zn_{MP}, Cu_{MP}, Cr_{MP} and Ni_{MP}, as observed in Fig. 2. The main river showed a decline in trace metal contents from the P01 to P02 (Table 2), and a slight variation until the outer station (P03) with a salinity of 36.2 g kg^{-1}. The mangrove channel presented slight variation for all trace metals in intermediary salinity. Along the bay area, Cu_{MP}, Ba_{MP} and Zn_{MP} exhibited low values in the particulate fractions, while the Co_{MP}, Cr_{MP}, Pb_{MP} and Ni_{MP} did not show a clear trend variation with high salinities. The overall mean contents of trace metals in the particulate fractions presented the following decreasing order: Ba_{MP} (190.9 ± 129.0 μg g^{-1}) > Zn_{MP} (97.6 ± 58.6 μg g^{-1}) > Cr_{MP} (47.9 ± 19.5 μg g^{-1}) > Cu_{MP} (17.6 ± 7.7 μg g^{-1}) = Ni_{MP} (17.6 ± 7.3 μg g^{-1}) > Pb_{MP} (12.6 ± 5.6 μg g^{-1}) > Co_{MP} (8.1 ±

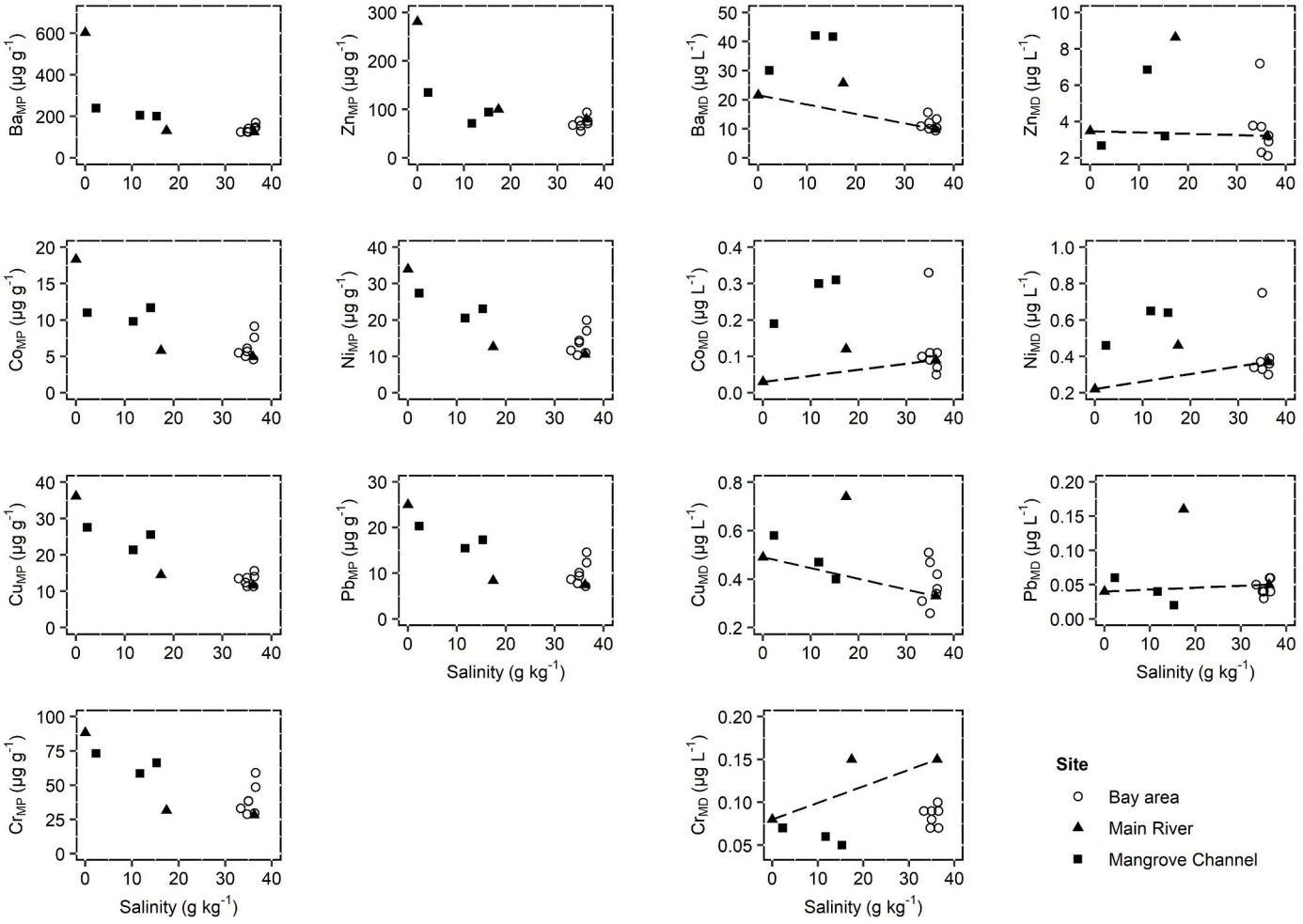

Fig. 2. Distribution of trace metals in the particulate fractions (μg g^{-1}) and dissolved fractions (μg L^{-1}) along the salinity gradients on the Parnaíba River Delta. Dashed line represents the theoretical dilution curve with the station P01 (salinity 0.0 g kg^{-1}) to station P03 (salinity 36.2 g kg^{-1}).

Table 1
Concentrations of trace metals in dissolved waters (μg L^{-1}), suspended particles (μg g^{-1}), and sediments (μg g^{-1}) along the Parnaíba River Delta.

Zone	Stations	Dissolved Metals (μg L^{-1})							Particulate Metals (μg g^{-1})							Sediments (μg g^{-1})						
		Ba	Zn	Co	Ni	Cu	Pb	Cr	Ba	Zn	Co	Ni	Cu	Pb	Cr	Ba	Zn	Co	Ni	Cu	Pb	Cr
Main river	**P01**	21.6	3.5	0.03	0.22	0.49	0.04	0.08	602.4	280.8	18.3	33.9	36.1	25.0	88.2	14.8	1.4	0.5	1.0	0.4	0.6	1.6
Main river	**P02**	25.6	8.6	0.12	0.46	0.74	0.16	0.15	131.5	99.9	5.8	12.6	14.5	8.4	31.6	15.5	2.0	0.6	1.3	0.4	1.0	2.7
Main river	**P03**	9.8	3.2	0.09	0.37	0.33	0.05	0.15	124.8	79.9	4.9	10.5	11.6	7.5	28.3	22.3	1.6	0.5	1.1	0.3	0.8	1.8
Mangrove channel	**P04**	30.0	2.7	0.19	0.46	0.58	0.06	0.07	239.0	134.9	11.0	27.4	27.6	20.3	73.2	84.2	21.7	5.6	8.7	7.9	6.6	29.8
Mangrove channel	**P05**	42.1	6.9	0.30	0.65	0.47	0.04	0.06	205.1	71.2	9.8	20.5	21.4	15.5	58.5	171.0	59.0	12.8	23.5	23.4	18.4	73.5
Mangrove channel	**P06**	41.7	3.2	0.31	0.64	0.40	0.02	0.05	200.2	94.3	11.7	23.1	25.5	17.3	66.3	120.5	48.2	10.2	18.6	17.5	14.2	56.9
Bay area	**P07**	11.0	3.8	0.10	0.34	0.31	0.05	0.09	124.9	67.8	5.5	11.6	13.5	8.7	33.1	81.2	33.8	6.8	13.2	9.9	10.0	47.2
Bay area	**P08**	10.0	2.3	0.09	0.33	0.26	0.03	0.09	141.3	66.5	6.1	14.3	13.7	10.1	38.7	–	–	–	–	–	–	–
Bay area	**P09**	15.7	7.2	0.33	0.37	0.51	0.04	0.07	126.9	76.4	5.0	10.3	12.4	7.8	29.0	146.4	59.8	10.7	24.1	19.7	17.2	69.9
Bay area	**P10**	12.2	3.7	0.11	0.75	0.47	0.04	0.08	125.6	55.5	5.7	13.9	11.3	9.5	38.4	135.1	52.7	9.4	23.3	19.1	16.4	66.5
Bay area	**P11**	9.4	2.1	0.05	0.30	0.34	0.06	0.10	142.4	94.3	4.6	11.0	11.3	7.2	29.7	121.1	50.6	9.7	21.0	15.6	15.5	64.2
Bay area	**P12**	13.4	2.9	0.11	0.39	0.36	0.04	0.07	147.8	71.3	9.1	19.9	15.7	14.6	59.0	94.3	41.1	7.8	16.7	12.5	13.2	52.7
Bay area	**P13**	10.3	3.2	0.07	0.36	0.42	0.06	0.09	169.7	76.2	7.6	17.0	14.1	12.3	48.6	–	–	–	–	–	–	–

3.2 μg g^{-1}). Spearman's rank ($p < 0.05$, $n = 13$) identified a significative negative correlation of Co_{MP}, Cu_{MP}, and Pb_{MP} with salinity ($r = -0.57$, -0.64, and -0.56, respectively) and pH ($r = -0.65$, -0.65, and -0.69, subsequently), and Ba_{MP} Cr_{MP}, and Ni_{MP} also exhibited negative correlation with pH ($r = -0.58$, -0.66, and -0.64, respectively). One-way ANOVA and Kruskal-Wallis tests identified no significant differences between almost all trace metals in the study area, except Cr ($p < 0.05$, $n = 13$).

3.3. Dissolved trace metal fractions

The dissolved trace metals along zones of PRD are demonstrated in Fig. 2. The dashed line represents the theoretical dilution curve between the two significative end members from the distinct water sources: freshwater zone at station P01 (salinity 0.0 g kg^{-1}) and the seawater zone at station P03 (salinity 36.2 g kg^{-1}). The metals exhibited a heterogeneous distribution, indicating non-conservative behavior along the PRD. In general, Ba_{MD} and Cu_{MD} have a decreasing trend and increase in salinity, while Cr_{MD} was the only element with high values with the increase of the salinity in the main river (P02 and P03). It is remarkable that the concentrations of all metals were above the theoretical dilution curve in the middle of the main river (P02) with a salinity of 17.4 g kg^{-1}. Ba_{MD}, Co_{MD} and Ni_{MD} had a tendency to increase in the mangrove channel at intermediary salinities (11.7 and 15.3 g kg^{-1}), while Cu_{MD}, Cr_{MD} and Zn_{MD} showed a decreasing tendency. Co_{MD}, Zn_{MD}, and Ni_{MD} also demonstrated high values at stations with high salinity in the bay area, such as P09 for the first two metals, and P10 for Ni_{MD}. Cu_{MD} did not exhibit a clear behavior in the bay area.

In general, the mean concentration of dissolved trace metals (Table 1) presented the following decreasing order: Ba_{MD} (19.4 ± 11.9 μg L^{-1}) > Zn_{MD} (4.1 ± 2.1 μg L^{-1}) > Cu_{MD} (0.44 ± 0.13 μg L^{-1}) > Ni_{MD} (0.43 ± 0.16 μg L^{-1}) > Co_{MD} (0.15 ± 0.10 μg L^{-1}) > Cr_{MD} (0.09 ± 0.03 μg L^{-1}) > Pb_{MD} (0.05 ± 0.03 μg L^{-1}). However, Spearman's correlation ($p < 0.05$, $n = 13$) indicate that most dissolved trace metals did not show significative variation with salinity gradient, except for Ba_{MD} with a negative correlation ($r = -0.76$). Ba_{MD} and Cr_{MD} also exhibited significative correlation with pH (r = - 0.8 and 0.7, respectively). The DOC exhibited a positive correlation only with Pb_{MD} ($r = 0.59$). Ba_{MD} also exhibited a positive correlation with Ba_{MP} ($r = 0.57$), while Cr_{MD} was negative correlated with Cr_{MP} (r = - 0.63). One-way ANOVA and Kruskal-Wallis tests identified significant differences for almost all elements in the dissolved fractions, except for Co_{MD}, Pb_{MD} and Zn_{MD} ($p > 0.05$, $n = 13$).

3.4. Surface sediments: textural characteristics and organic matter

The spatial variation of grain-size showed a diverse hydrodynamic system along the PRD, with sand representing the main fraction. The main river was composed totally of sand (100%) with no fine-grained fraction (0.0%). The mangrove channel and bay area were more heterogeneous compared to the sediments from the river, with the highest values of the fine-grained fraction at 21.7 and 23.3% in the stations P04 and P07, respectively. The sediment grain-sizes of the PRD were composed of a sand fraction with 89.2 ± 8.1% (76.7–100.0%), and a fine grain-sized fraction with an average value of 10.8 ± 8.1% (0.0–23.3%). Spearman's correlation ($p < 0.05$, $n = 11$) showed that the sand and fine-grained fraction had a negative correlation between them ($r = -0.99$). The OM% was more enriched in the sediments of the mangrove channel and bay area, with the highest values at stations P09 and P10, reaching 17.5 and 20.5%, respectively, and located more distant from the mouth of bays. Low percentages were observed in all stations of the main river, with sediments composed of sand, mainly at station P03 with 0.1%. The OM% in the sediments was 9.5 ± 7.5% (Table S2). Spearman's correlation ($p < 0.05$, $n = 11$) showed that the OM and DOC presented a negative correlation between them ($r = -0.81$). Shapiro-Wilk test identified normal distributions for sand, fine-

Table 2
Log (Kd) of trace metals among the estuarine compartments around the world. MS, MD, MP, and MPw means trace metal in the sediments, dissolved fractions particulate fractions, and porewater, respectively.

References	Environment	Fractions	Log (Kd)						
			Ba	Cr	Co	Cu	Ni	Pb	Zn
Present study	Parnaíba River Delta (Brazil)	MP/MD	4.1	5.8	4.9	4.7	4.7	5.5	4.5
		MS/MD	3.3	5.2	4.1	3.7	4.0	4.7	3.3
Allison and Allison (2005)	EPA (models)	MS/MPw	2.8	4.9	3.1	3.5	3.9	4.6	4.1
		MP/MD	4.0	4.5	4.7	4.2	4.0	5.1	3.7
Fu et al. (2013)	East-Hainan Rivers (China)	MP/MD	–	–	5.3	4.8	5.1	5.7	–
La Colla et al. (2015)	Bahía Blanca estuary (Argentina)	MP/MD	–	2.8	–	3.3	2.9	2.8	3.3
Wang and Wang (2016)	Jiulong River Estuary (China)	MP/MD	–	5.1	–	4.4	3.8	6.0	4.8
Luengen et al. (2007)	San Francisco Bay (USA)	MP/MD	–	–	4.7	4.1	4.5	5.9	5.2
Ollivier et al. (2011)	Rhône River (France)	MP/MD	4.0	–	–	4.3	4.6	5.8	4.8
Liu et al. (2019)	Pearl River (China)	MS/MD	–	–	–	–	–	4.8	5.6
Pavoni et al. (2021)	Northern Adriatic Sea (Italy)	MS/MD	4.0	5.5	5.1	4.3	5.0	4.8	4.5

grained fraction, and OM% in the sediments ($p > 0.05$), while Bartlett's test did not show their homogeneity of variances ($p < 0.05$). Kruskal-Wallis test observed significant differences for the grain-size and OM in the sediments along the zones ($p > 0.05$).

3.5. Total contents of trace metals in the surface sediments

The contents of trace metals (Table 1) in the surface sediments show a heterogeneous spatial distribution, where the main river exhibited the lowest contents for Ba_{MS}, Cr_{MS}, Ni_{MS}, PbM_S and Zn_{MS} with the values of 14.8, 1.6, 1.0, 0.6 and 1.5 μg g^{-1} respectively, at station P01. Station P03 presented the minimum values for Cu_{MS} (0.3 μg g^{-1}) and Co_{MS} (0.5 μg g^{-1}). The highest contents for Ba_{MS}, Cr_{MS}, Co_{MS}, Cu_{MS} and Pb_{MS} were observed at station P05 in the mangrove channel (171.0, 73.5, 12.8, 23.4 and 18.4 μg g^{-1}, respectively), and in the bay area, Ni (24.1 μg g^{-1}) and Zn (59.8 μg g^{-1}) were higher at station P09. The mean contents of trace metals in the sediments presented the following decreasing order: Ba_{MS} (91.5 ± 54.4 μg g^{-1}) > Cr_{MS} (42.4 ± 28.6 μg g^{-1}) > Zn_{MS} (33.8 ± 23.3 μg g^{-1}) > Ni_{MS} (13.9 ± 9.4 μg g^{-1}) > Cu_{MS} (11.5 ± 8.4 μg g^{-1}) > Pb_{MS} (10.4 ± 7.0 μg g^{-1}) > Co_{MS} (6.8 ± 4.5 μg g^{-1}), different from the trace metals in the particulate fractions. One-way ANOVA and Kruskal-Wallis tests identified no significant differences for almost all elements in the surface sediments, except for Ba_{MS} and Cu_{MS}, ($p > 0.05$, $n = 11$). Spearman's rank demonstrates that OM% had a positive correlation with all trace metals in the sediments, where Ba_{MS}, Cr_{MS}, Zn_{MS}, Ni_{MS}, Pb_{MS}, Cu_{MS} and Co_{MS} showed the values of $r = 0.82$, 0.85, 0.88, 0.88, 0.85, 0.85, 0.80, respectively. Additionally, Co_{MD} was positively correlated with Co_{MS} ($r = 0.62$), and Zn_{MP} was negatively correlated with Zn_{MS} ($r = 0.60$).

3.6. Distribution coefficient (Log (Kd))

The distribution coefficient of trace metals between the particulate and dissolved fractions (Log $(Kd)_{MP/MD}$) exhibited higher mean values than trace metal concentrations in sediments and dissolved fractions (Log $(Kd)_{MS/MD}$). The mean values for Log $(Kd)_{MP/MD}$ were observed in the decreasing order: Cr (5.7) > Pb (5.4) > Co (4.8) > Ni (4.6) = Cu (4.6) > Zn (4.4) > Ba (4.0); and Log $(Kd)_{MS/MD}$: Cr (5.4) > Pb (5.1) > Co (4.5) > Ni (4.3) > Cu (3.7) = Zn (3.7) > Ba (3.6). The Wilcoxon test identified no significant difference between the mean values of Log $(Kd)_{MP/MD}$ and Log $(Kd)_{MS/MD}$ for almost all trace metals, except Ba and Zn ($p > 0.05$). Log $(Kd)_{MP/MD}$ exhibited no significant differences for almost all trace metal along the zones, except for Cr ($p < 0.05$, $n = 13$). While, Log $(Kd)_{MS/MD}$ evidenced significant differences for the all the metals ($p < 0.05$, $n = 11$) (Fig. 3 and Table S3).

Ba, Zn, and Cu displayed weak associations with the solid phase (3< Log (Kd) < 5) for both coefficients. However, the Log $(Kd)_{MS/MD}$ of Ba and Cu exhibited a preference for the liquid phase at stations P01 and P02, and for Zn at all stations of the main river. Pb and Cr showed an affinity to bind or remain in a solid phase (Log (Kd) ≥ 5) for both coefficients. Nevertheless, Log $(Kd)_{MP/MD}$ of Pb presented a weak association with the solid phase at station P02, as well as Log $(Kd)_{MS/MD}$ of Pb and Cr at all stations of the main river (3< Log (Kd) < 5). Ni and Co presented weak associations with the solid phase in both coefficients

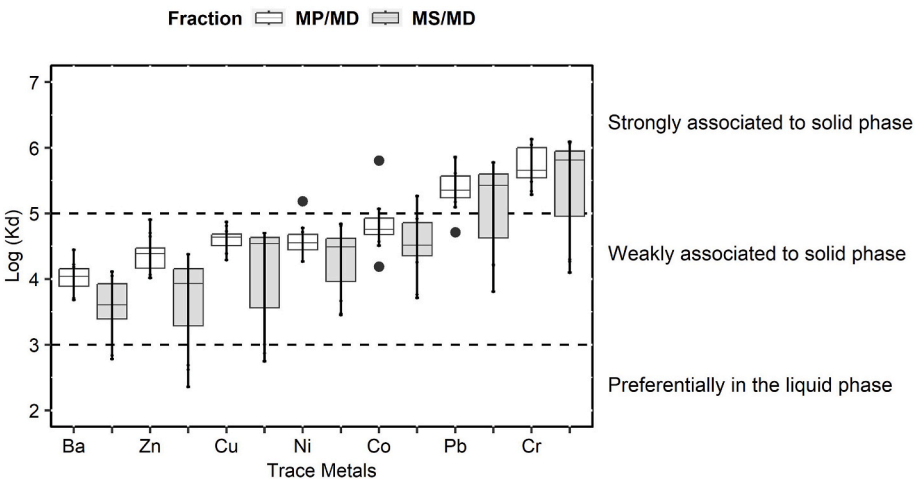

Fig. 3. Box–Whisker plots of Log (Kd) of particulate with dissolved fractions (MP/MD) and sediments with dissolved fractions (MS/MD) for the studied metals along the Parnaíba River Delta. Median values are the bold bars (—) with quartiles 0.25 and 0.75 in boxes; horizontal bars represent the 25% and 75% interval; and (●) correspond to outlier values.

(3< Log (Kd) < 5). However, Log $(Kd)_{MP/MD}$ for Ni and Co displayed a stronger preference for the particulate fractions at station P01 of the main river, and at station P13 of the bay area in the case of Co. Also, Log $(Kd)_{MS/MD}$ for Co showed strongly associated with the solid phase at station P11 in the bay area.

The PCA was applied to observe the influence of the salinity, pH, DOC and SPM on the Log $(Kd)_{MP/MD}$ of the elements along the PRD's zones (Fig. 4). It accounted for 68.0% of the total variance that explained metal partition along the zones. Factor 1 explains the 44.9% of the total variance and presents high loading values for Log $(Kd)_{MP/MD}$ of Cu, Ni, Pb, Cr and Zn, while Factor 2 explains 23.1% of the total variance, indicating that salinity and pH have an inverse influence on the Log $(Kd)_{MP/MD}$. DOC and SPM did not show a significant influence on the trace metal partitioning in the subsurface waters. The PCA also suggests that the behavior of variables in the subsurface waters from the main river and bay area are more similar between them, while the mangrove channel showed different processes in trace metal partitioning compared to the rest of the environment.

It was also applied the PCA for the Log $(Kd)_{MS/MD}$ of trace metals, textural characteristics and OM from the surface sediments, that accounted for 94.0% of the total variance. Factor 1 explains 83.5% of the total variance, indicating that OM and fine-grained fraction have an influence on the Log $(Kd)_{MS/MD}$ of all trace metals partitioning in the mangrove channel and bay area of PRD. In addition, Factor 2 explains 10.5.% of the total variance, exhibiting sand with negative influence on the fine-grained. Observe the variables characterized for the surface sediments present similarity between mangrove channel and bay area, while the main river presents a distinct pattern. The different similarities between zones with the trace metals in the subsurface waters and surface sediments evidencing the distinct processes of trace metal partitioning along the compartments.

3.7. Environmental index quality

The results of Igeo are presented in Fig. 5 and Table S3. In general, the anomalous values were higher for trace metal contents in the particulate fractions than in the surface sediments, as observed in the decreasing order of the Igeo values in the particulate fractions: Zn (2.1) > Cr (0.7) = Cu (0.7) > Pb (0.4); and in the sediments: Pb (0.1) > Zn (−0.2) > Cr (−0.3) > Cu (−0.9). Nevertheless, Wilcoxon test identified no significant difference of Igeo values between the compartments for almost all trace metals, except Zn ($p > 0.05$).

All metals in the sediments were classified as uncontaminated (Class 0) in the stations of main river. Zn exhibited the lowest environmental quality in the particulate fractions, classifying as heavily contaminated at station P01 (Class 4) and moderated to heavily contaminated at stations P02, P03, P04, P06 and P011 (Class 3). The classification for Zn in the surface sediments indicate moderately contamination (Class 2) in almost all locations, while P04 and P07 was identified as uncontaminated classification (Class 0). The other trace metals exhibited similar Igeo classification, with moderate contamination (Class 2) for Pb_{MS}, and uncontaminated to moderately contaminated (Class 1) for both solid phase of particulate fractions and sediments for Cu and Cr.

4. Discussion

4.1. Environmental conditions

The high-water temperatures observed in PRD are common in equatorial estuaries due to the solar radiation is nearly continuous throughout the year. Similar temperature values have been reported in other studies in estuaries of Northeast Brazil (Dias et al., 2016; Serejo et al., 2020). The main river exhibits a typical longitudinal salinity and pH gradient due to the mixing process between the freshwater and the seawater forces. The interaction between these different waters changes the variability of the physicochemical variables and the partitioning of trace metals along the PRD. The initial slightly alkaline pH of freshwater at station P01 (pH 7.4) in the main river gradually increased to more alkaline conditions to outer station P03 (pH 8.1). This pH change occurred due to the high concentrations of carbonate and bicarbonate ions present in seawater with high salinity (Machado et al., 2016). The mangrove channel had low pH values due to freshwater influence, which probably has a lower hydrodynamic influence compared to the bay area and main channel of the river. Additionally, the low pH values may be the result of degradation of OM by microorganisms (Millero, 2013). The bay area showed strong seawater influences in the subsurface waters with homogenous values for salinity and alkaline pH.

The sampling realized in the present study only gives a snapshot of geochemical processes. However, it was observed that the primary pathway for trace metals in the PRD is associated with the particulate fractions due to elevated contents. The high values in the upstream of the environment occur due to weathering in the drainage basin that

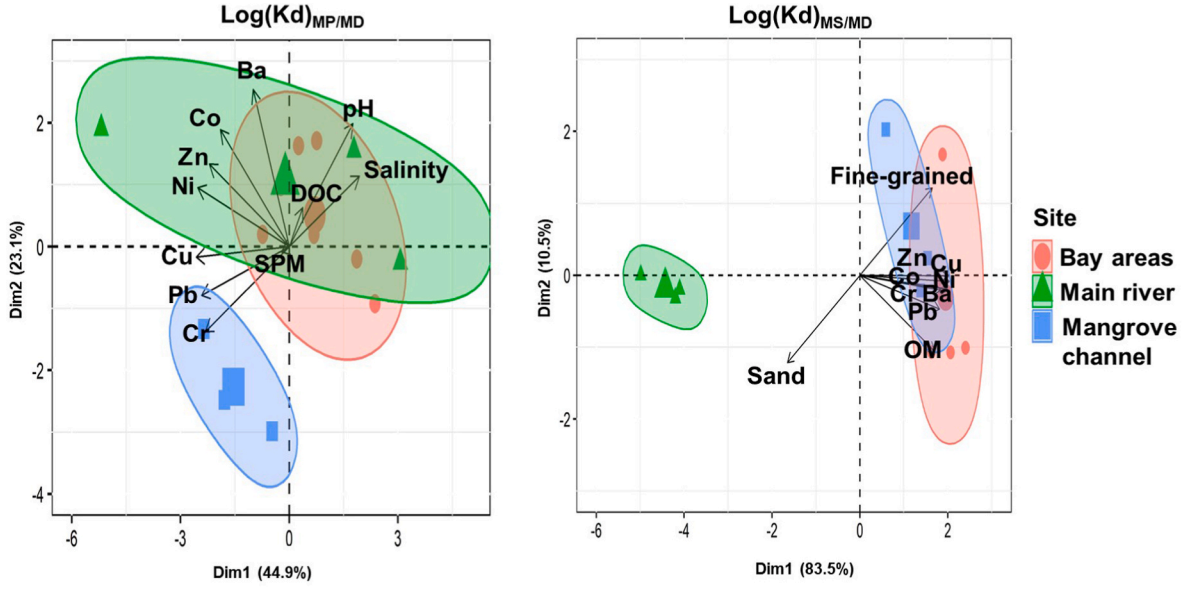

Fig. 4. Principal component analysis (PCA) with distribution coefficients Log (Kd) of trace metals (Ba, Cr, Co, Cu, Ni, Pb and Zn) with a) physicochemical variables in the subsurface waters and b) surface sediments characteristics along the zones on the Parnaíba River Delta.

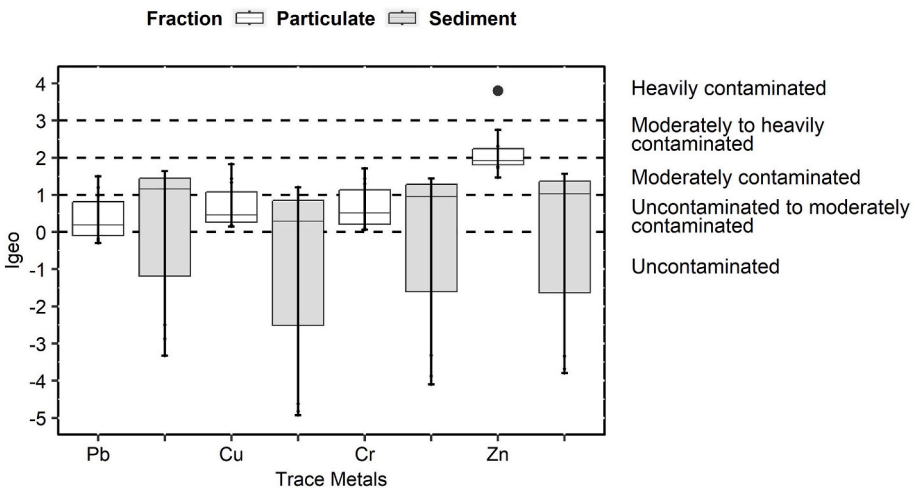

Fig. 5. Box–Whisker plots of geoaccumulation index (Igeo) for the trace metals in the particulate fractions and surface sediments in the Parnaíba River Delta. Median values are the bold bars (—) with quartiles 0.25 and 0.75 in boxes; horizontal bars represent the 25% and 75% interval; and (●) correspond to outlier values.

transports the metals to the PRD in the SPM, predominantly from the lithogenic origin linked to the residual fraction of the material. The decrease of SPM in the main river may occur due to the reduction in river discharges characteristic of the dry season during intensified periods of drought in this equatorial region (Cavalcante et al., 2021). This condition, in conjunction with the flood tide, tends to decrease the SPM transport along the estuary. The increment of SPM in the mangrove channel during the change from ebb to flood tidal phases may be related to the presence of a bottom saline front in the stations P05 and P06 that cause margin erosion (dos Santos et al., 2020).

The bay area presents similar values of SPM compared to the other zones, except for the high value observed at station P12 under ebb tide. The high value of SPM is a consequence of margin erosion and resuspension of bank sediment that is pulled out of the delta during the ebb tide (Aquino da Silva et al., 2019; Diasda et al., 2016). This variation in SPM was also observed in previous studies in the area and other coastal environments in Northeast Brazil (Aquino da Silva et al., 2019; Serejo et al., 2020).

The OM in the sediments acts as an important geochemical carrier of contaminants in the PRD, while DOC in the subsurface waters showed influence only for Pb_{MD}. OM can bind contaminants in estuarine environments due to functional groups that bound with trace metals through the formation of ionic or covalent bonds, which can release them by the change in pH (Alkhatib et al., 2016). This influence of OM was also observed in the sediments of other Amazonian estuaries of northeastern Brazil (Santos et al., 2019).

To better comprehension of the behavior of trace metals along the PRD, it was decided to discuss the elements in groups observed in the PCA from the Log $(Kd)_{MP/MD}$, such as Ba, Zn–Co–Ni, and Cu–Cr– Pb.

4.2. Barium partitioning

The positive correlation observed between Ba_{MP} and Ba_{MD} may suggest a constant desorption and adsorption process within the environment. However, a noticeable transfer of Ba_{MP} to Ba_{MD} occurs under the increasing salinity, ranging from 0.0 g kg^{-1} at station P01 to 17.5 g kg^{-1} in station P02 of the main river, and a salinity gradient from 2.3 g kg^{-1} at station P04 to 11.7 g kg^{-1} at station P05 of the mangrove channel. The weak association of Ba with solid phases contributes to the easy release of Ba_{MP} to liquid phase in the subsurface waters. This desorption phenomenon happens due to the high ionic strength and the presence of anions and cations present in the seawater, which tend to desorb the trace elements from particles (Gaulier et al., 2021). The behavior of Ba at PRD is in agreement with environments around the world under a salinity gradient (Coffey et al., 1997; Mori et al., 2019).

The low values of Ba_{MP} and Ba_{MD} in the bay area may be associated with the strong influence of salinity to induce the flocculation, settling the metal to the bottom. Ba has a larger ionic radius and lower hydration energy that facilitates the adsorption to SPM, and also can be bound to sulfate to low soluble form ($BaSO_4$) that precipitates and removes Ba from the subsurface waters (Wang et al., 2021). The mean value of Log $(Kd)_{MP/MD}$ and Log $(Kd)_{MS/MD}$ displayed a significant difference between them, evidencing the distinct geochemical processes affecting the behavior of Ba in the environmental compartments of PRD, as mentioned previously. The mean value Log $(Kd)_{MP/MD}$ determined for Ba in PRD was slightly higher than the results of geochemical speciation found in the literature (Table 2).

4.3. Zinc, cobalt and nickel partitioning

The group composed of Zn, Co and Ni exhibits the same primary pathway associated with the particulate fractions in the subsurface waters of the main river, removed by the salinity and pH elevation. In the case of Zn_{MP}, the decrease may occur due to the desorption from particulate to dissolved fractions. Zn_{MP} was the only metal with a bad quality index, classified as heavily contaminated at station P01 (Class 4) and moderately to heavily contaminated at stations P02, P03, P04, P06 and P11 (Class 3). This contamination was less pronounced in the sediments with a classification of uncontaminated to moderate contaminated (Class 2). The enrichment of Zn is related to anthropic activities, such as untreated domestic effluent and livestock activities occurred in the main regional urban center of Parnaíba city, followed by a natural contribution from weathering of soils (Paula Filho et al., 2021, 2015; 2014).

Although, due to the local high hydrodynamic characteristics of this region (Aquino da Silva et al., 2019, 2015), which influence the dominance of sand in the sediments, adsorption is impeded by the low specific surface area and absence of OM contents in the main river (Kouassi et al., 2019). Another study in PRD identified Zn_{MS} bound to labile fractions, such as the exchangeable and carbonates, displaying a medium mobility risk level to the environment (Alves, 2022). The positive correlation of Zn_{MS} with OM contents can immobilize it to the bottom, but can be released to soluble species in PRD under the changes in redox conditions. This collaborates with the weak association with the solid phase identified for both Log (Kd) values. Similar behavior for Zn was observed in tropical estuarine sediments of Ebrie Lagoon in Ivory Coast (Kouassi et al., 2019). Nabelkova and Kominkova (2012) also identified Zn as the most available and hazardous in most urbanized Prague creeks

from heavy traffic areas in the drainage basin. Zn is essential for the development of plants and animals, but in high concentrations, can cause harmful effects to the aquatic biota (Ma et al., 2020; Wu et al., 2019).

The correlation between Ni and Co and their similar distribution in the fractions of the subsurface waters and surface sediments of PRD may suggest a common source and geochemical process on their partitioning. Salinity and pH also play an important influence in the desorption of Ni_{MP} and $Co_{MP,}$ as observed for the previous metals discussed. The transfer to the dissolved fractions occurred at station P02 in the main river, in the all stations of the mangrove channel, and stations P10 for Ni_{MD} and P09 for Co_{MD} in the bay area.

Ni and Co exhibited Log $(Kd)_{MP/MD}$ and Log $(Kd)_{MS/MD}$ with a weak association with the solid phase, and also displayed a strong association with the solid phase. The preference of Ni for the particulate fraction at station P01 collaborates with the idea that the primary source of Ni originates from lithogenic sources, which are bound to the residual fraction of the SPM. While, the strong association of Co with the solid phases observed in the station P11 for Log $(Kd)_{MS/MD}$, and P13 for Log $(Kd)_{MP/MD}$ indicates that Co is present in more stable compounds on the solid phases (Sedeño-Díaz et al., 2019).

The positive correlation between Co_{MS} and Co_{MD} indicates that the sediments can work as a secondary source of Co to the subsurface waters. The trace metals in the sediments of PRD can suffer diagenesis due to temperatures, biological activities and redox conditions that remobilize the contaminates (Duan et al., 2019). When Co is found bound to Fe–Mn oxides, it can be mobilized from the sediments to the water compartment under reductive conditions, as observed in the Modaomen estuary (China) (Jia et al., 2021). However, the solubility of Co to dissolved fractions in PRD is associated with Co_{MS} bound to OM, which releases the trace metals in response to changes in redox conditions during seawater intrusion (Duan et al., 2019; Machado et al., 2016). Both Log (Kd) for Co and Ni in PRD were systematically higher than determined by EPA (Table 2), while Log $(Kd)_{MS/MD}$ Zn was lower when compared to the EPA and Pearl River in China (Liu et al., 2019). It may suggest more mobility of trace metals from solid-phase to subsurface waters in PRD than in other coastal environments. The no clear trend of Ni_{MP} and Co_{MP}, in the bay area of PRD may be related to margin erosion that resuspend these elements bound to different fractions from the sediments.

4.4. Copper, chromium and lead partitioning

The last group demonstrates that Cu_{MP} and Pb_{MP} have a negative correlation with salinity and pH, and Cr_{MP} is negatively correlated with pH along the PRD. For Cu, the dominant partitioning process is desorption caused by seawater intrusion in estuary mixing zones, evident from the significant number of stations positioned above the theoretical dilution curve in Fig. 2. It collaborates with both Log (Kd) for Cu, with weak association to solid-phase for almost all stations, and the stations P01 and P02 showed preference of Log $(Kd)_{MS/MD}$ in the liquid phase. The increase of Cu_{MD} due to mobilization from particulate fractions was also observed in Jiulong River Estuary, China (Wang and Wang, 2016). Cu usually exhibits a significant association with colloidal and dissolved organic matter in the subsurface waters, that degrades with seawater intrusion, leading to an increase in this contaminant in the dissolved fractions (Mosley and Liss, 2019; Regnier and Wollast, 1993). Also, Cu in PRD can be derived from anthropogenic sources, such as urban runoff, improper solid waste disposal, agriculture and shrimp farming, as identified by the emission factors (Paula Filho et al., 2014).

In general, the results showed low enrichment of this contaminant to the solid phase, classified as uncontaminated to moderately contaminated for Cu_{MP} (Class 1), and uncontaminated for Cu_{MS} (Class 0). This can be explained by the dominant presence of Cu_{MS} bound to the residual fraction and secondly with OM, as exhibited by the sequential extraction conducted on the surface sediments of PRD (Alves, 2022).

The spatial distribution of Pb and Cr in the particulate and dissolved fractions indicate a dominant removal from the subsurface waters to the sediments, except some stations of the bay area. Pb usually exhibits high particle reactivity (Gaulier et al., 2021; Wang and Wang, 2016), and Cr_{MD} usually undergoes precipitation in alkaline pH (de Souza Viana et al., 2023). DOC showed as an important geochemical carrier for Pb_{MD} in PRD. Similar influence was observed in Jiulong River Estuary, China as described by Wang et al. (2017). Where OM in both colloidal and particulate fractions were responsible for effectively binding and regulating Pb during the mixing process. Also, the immobility of Pb and Cr can be explained by their binding to the residual fractions and to the Fe–Mn oxides under oxic conditions from the seawater (Domingos et al., 2015; Omanovic et al., 2015; Santos et al., 2019).

Whereas, the heterogenous variation of Pb_{MP} and Cr_{MP} can be also associated with sediment resuspension in bay area, as observed for Ni_{MP} and Co_{MP}. These results are in agreement with emission factors determined in the Parnaíba River Basin, which Pb and Cr were mainly from natural weathering in the drainage basin (Paula Filho et al., 2014). Notwithstanding, Log $(Kd)_{MP/MD}$ for Cr and Pb, and Log $(Kd)_{MS/MD}$ for Cr demonstrated that these elements were not a big concern for the quality of the environment due to strong association to solid phases, corroborating with Igeo classification of uncontaminated for Cr_{MS}, and uncontaminated to moderately contaminated for Cr_{MP} and Pb in both solid phases.

Log $(Kd)_{MP/MD}$ for Cu, Cr and Pb in PRD also presented higher values (Table 2) than determined by EPA and other estuaries influenced anthropogenically (Allison and Allison, 2005; La Colla et al., 2015), while in Log $(Kd)_{MS/MD}$ more mobility due to the slight lower values when compared to the other estuaries (Allison and Allison, 2005; Pavoni et al., 2021). The distinct trace metal partitioning evidencing the complex variability of the geochemical processes of fate and mobilization influenced by the physicochemical parameter variation and the characteristic of surface sediments along the zones of the PRD.

5. Conclusion

The present study provides information about the dynamic of metal partitioning in the subsurface waters (particulate and dissolved fractions) and sediments the along the zones of PRD in dry season and during the spring tide effect. The trace metals have the primary pathway associated to the SPM, that suffers removal from this fraction under the influence of the increase in salinity and pH. Ba_{MP}, Zn_{MP}, Ni_{MP}, Co_{MP}, Cu_{MP} suffers desorption to the dissolved fractions, while Pb_{MP} and Cr_{MP} demonstrate precipitation to the surface sediments. The values of Log $(Kd)_{MP/MD}$ and Log $(Kd)_{MS/MD}$ suggest a potential mobilization of Ba, Zn and Cu from solid phase to dissolved species, and Pb and Cr do not present this concern due to the strong association with the particulate fractions and sediments. OM plays an important role as a geochemical carrier, binding the trace metals to the bottom sediments, and for Pb_{MD} in the subsurface waters. High values of Zn in the particulate fractions indicated by Igeo suggest enrichment from anthropogenic activities. These findings not only contribute to our understanding of ecological risks posed by metal contamination, but also provide insights for global pollution mitigation in coastal tidal estuaries, particularly those characterized by intensive physical mixing along equatorial coasts.

Funding

Dr. SANTOS was funded by the CAPES/PrInt (N° 03/2019). Dr. MARINS has received research support from the PRONEX/FUNCAP/CNPq (Proc. N° PR2-0101-00052.01.00/15). Dr. MOUNIER was funded by the Franco-Brazilian research program COFECUB (N° 44994 YE).

CRediT authorship contribution statement

Thays Thayanne Luz Santos: Writing – review & editing, Writing –

original draft, Visualization, Validation, Methodology, Investigation, Formal analysis, Data curation, Conceptualization. **Jean Louis Stéphane Mounier:** Writing – review & editing, Writing – original draft, Supervision, Resources, Methodology, Funding acquisition, Conceptualization. **Rozane Valente Marins:** Writing – review & editing, Writing – original draft, Supervision, Resources, Methodology, Funding acquisition, Conceptualization.

Declaration of competing interest

The authors declare that they have no known competing financial interests or personal relationships that could have appeared to influence the work reported in this paper.

Data availability

Data will be made available on request.

Acknowledgement

The Authors would like to thank for the Dr. Dario Omanović from the Center for Marine and Environmental Research (Ruđer Bošković Institute-Croatia) for the analyses.

Appendix A. Supplementary data

Supplementary data to this article can be found online at https://doi.org/10.1016/j.envpol.2024.123500.

References

Alkhatib, E.A., Grunzke, D., Chabot, T., 2016. Multi-regression Prediction of metal partition coefficients under various physical/chemical Conditions"Design of experiments as, Cr, Cu, Ni and Zn.". Hydrol. Curr. Res. 7, 1–7. https://doi.org/10.4172/2157-7587.1000241.

Allison, J.D., Allison, T.L., 2005. Partitioning coefficients for metals in surface water, soil and waste. U.S. Environ. Prot. Agency. Off. Res. Dev.1-93. URL https://cfpub.epa.gov/si/si_public_record_report.cfm?Lab=NERL&dirEntryId=135783.

Alves, L.P., 2022. Distribuição e fracionamento geoquímico de metais em sedimentos superficiais do Delta do Rio Parnaíba (Graduation monography). Univ. Fed. do Ceará. Fortaleza, Brazil.1-48. URL http://www.repositorio.ufc.br/handle/riufc/70904.

Aquino da Silva, A.G., Amaro, V.E., Stattegger, K., Schwarzer, K., Vital, H., Heise, B., 2015. Spectral calibration of CBERS 2B multispectral satellite images to assess suspended sediment concentration. ISPRS J. Photogrammetry Remote Sens. 104, 53–62. https://doi.org/10.1016/j.isprsjprs.2015.02.011.

Aquino da Silva, A.G., Stattegger, K., Vital, H., Schwarzer, K., 2019. Coastline change and offshore suspended sediment dynamics in a naturally developing delta (Parnaíba Delta, NE Brazil). Mar. Geol. 410, 1–15. https://doi.org/10.1016/j.margeo.2018.12.013.

Bianchi, T.S., 2007. Biogeochemistry of Estuaries. OXFORD University Press, New York.

Cavalcante, M.S., Marins, R.V., Dias, F.J. da S., Rezende, C.E. de, 2021. Assessment of carbon fluxes to coastal area during persistent drought conditions. Reg. Stud. Mar. Sci. 47, 101934 https://doi.org/10.1016/j.rsma.2021.101934.

Chielle, R.S.A., Marins, R.V., Cavalcante, M.S., Cotovicz Jr., L.C., 2023. Seasonal and spatial variability of CO2 emissions in a large tropical mangrove-dominated delta. Limnol. Oceanogr. Oceanogr. 12471 https://doi.org/10.1002/lno.12471.

CHN, 2019. Porto de Luís correia (estado do Piauí) - 2019. Cent. Hidrogr. da Mar. URL https://www.marinha.mil.br/chm/tabuas-de-mare (accessed 12.1.19).

Coffey, M., Dehairs, F., Collette, O., Luther, G., Church, T., Jickells, T., 1997. The behaviour of dissolved barium in estuaries M. Estuarine, coast. ShelfScience 45, 113–121. https://doi.org/10.2307/2786886.

Costa, F.W.D., 2019. Aspectos geográficos e a gestão de ambientes costeiros: um enfoque na Resex do Delta do Parnaíba. Rev. Geociências do Nord 5, 1–16. https://doi.org/10.21680/2447-3359.2019v5n0id18406.

de Souza Viana, L.M., Constantino, W.D., Tostes, E.C.L., Luze, F.H.R., de Barros Salomão, M.S.M., de Jesus, T.B., de Carvalho, C.E.V., 2023. Seasonal variation, contribution and dynamics of trace elements in the drainage basin and estuary of the Serinhaém river. BA. Mar. Pollut. Bull. 188 https://doi.org/10.1016/j.marpolbul.2023.114653.

Dias, F.J. da S., Castro, B.M., Lacerda, L.D., Miranda, L.B., Marins, R.V., 2016. Physical characteristics and discharges of suspended particulate matter at the continent-ocean interface in an estuary located in a semiarid region in northeastern Brazil. Estuar. Coast Shelf Sci. 180, 258–274. https://doi.org/10.1016/j.ecss.2016.08.006.

Diniz, C., Cortinhas, L., Nerino, G., Rodrigues, J., Sadeck, L., Adami, M., Souza-Filho, P. W.M., 2019. Brazilian mangrove status: three decades of satellite data analysis. Rem. Sens. 11 https://doi.org/10.3390/rs11070808.

Domingos, R.F., Gélabert, A., Carreira, S., Cordeiro, A., Sivry, Y., Benedetti, M.F., 2015. Metals in the aquatic environment — interactions and implications for the speciation and bioavailability : aquat. Geochemistry 21, 231–257. https://doi.org/10.1007/s10498-014-9251-x.

dos Santos, V.H.M., da Silva Dias, F.J., Torres, A.R., Soares, R.A., Terto, L.C., de Castro, A.C.L., Santos, R.L., Cutrim, M.V.J., 2020. Hydrodynamics and suspended particulate matter retention in macrotidal estuaries located in Amazonia-semiarid interface (Northeastern-Brazil). Int. J. Sediment Res. 35, 417–429. https://doi.org/10.1016/j.ijsrc.2020.03.004.

Duan, L., Song, J., Liang, X., Yin, M., Yuan, H., Li, X., Ren, C., Zhou, B., Kang, X., Yin, X., 2019. Dynamics and diagenesis of trace metals in sediments of the Changjiang Estuary. Sci. Total Environ. 675, 247–259. https://doi.org/10.1016/j.scitotenv.2019.04.190.

FAO, 2020. Mangrove management: distribution and extent. Food Agric. Organ. United Nations. URL http://www.fao.org/forestry/mangrove/3643/en/ (accessed 3.25.21).

Folk, R.L., Ward, W.C., 1957. Brazos River bar: a study in the significance of grain size parameters. J. Sediment. Petrol. 27, 3–26. https://doi.org/10.1306/74D70646-2B21-11D7-8648000102C1865D.

Fu, J., Tang, X.L., Zhang, J., Balzer, W., 2013. Estuarine modification of dissolved and particulate trace metals in major rivers of east-hainan, China. Continent. Shelf Res. 57, 59–72. https://doi.org/10.1016/j.csr.2012.06.015.

García-Martín, E.E., Sanders, R., Evans, C.D., Kitidis, V., Lapworth, D.J., Rees, A.P., Spears, B.M., Tye, A., Williamson, J.L., Balfour, C., Best, M., Bowes, M., Breimann, S., Brown, I.J., Burden, A., Callaghan, N., Felgate, S.L., Fishwick, J., Fraser, M., Gibb, S.W., Gilbert, P.J., Godsell, N., Gomez-Castillo, A.P., Hargreaves, G., Jones, O., Kennedy, P., Lichtschlag, A., Martin, A., May, R., Mawji, E., Mounteney, I., Nightingale, P.D., Olszewska, J.P., Painter, S.C., Pearce, C. R., Pereira, M.G., Peel, K., Pickard, A., Stephens, J.A., Stinchcombe, M., Williams, P., Woodward, E.M.S., Yarrow, D., Mayor, D.J., 2021. Contrasting estuarine processing of dissolved organic matter derived from natural and human-impacted landscapes. Global Biogeochem. Cycles 35, 1–17. https://doi.org/10.1029/2021GB007023.

Gaulier, C., Zhou, C., Gao, Y., Guo, W., Reichstädter, M., Ma, T., Baeyens, W., Billon, G., 2021. Investigation on trace metal speciation and distribution in the Scheldt estuary. Sci. Total Environ. 757, 143827 https://doi.org/10.1016/j.scitotenv.2020.143827.

Godoy, M.D.P., Lacerda, L.D. de, 2014. River-island morphological response to basin land-use change within the Jaguaribe river estuary, NE Brazil. J. Coast Res. 30, 399–410. https://doi.org/10.2112/JCOASTRES-D-13-00059.1.

Guillén, M.T., Delgado, J., Albanese, S., Nieto, J.M., Lima, A., De Vivo, B., 2012. Heavy metals fractionation and multivariate statistical techniques to evaluate the environmental risk in soils of Huelva Township (SW Iberian Peninsula). J. Geochem. Explor. 119–120, 32–43. https://doi.org/10.1016/j.gexplo.2012.06.009.

Guimarães-Costa, A.J., Machado, F.S., Oliveira, R.R.S., Silva-Costa, V., Andrade, M.C., Giarrizzo, T., Saint-Paul, U., Sampaio, I., Schneider, H., 2019. Fish diversity of the largest deltaic formation in the Americas - a description of the fish fauna of the Parnaíba Delta using DNA Barcoding. Sci. Rep. 9, 1–8. https://doi.org/10.1038/s41598-019-43930-z.

Guzzi, A., 2012. Biodiveridade Do Delta Do Parnaíba, Biodiversidade Do Delta Do Parnaíba, Litoral Piauiense. EDUFPI, Parnaíba. https://doi.org/10.1017/CBO9781107415324.004.

IBGE, 2020. Paronama . Inst. Bras. Geogr. e Estatística IBGE. URL. https://cidades.ibge.gov.br/brasil/panorama (accessed 4.20.20).

INMET, 2020. Normal climatológica d climatológica do brasil 1981-2010. Inst. Nac. Meteorol. URL.

Jia, Z., Li, S., Liu, Q., Jiang, F., Hu, J., 2021. Distribution and partitioning of heavy metals in water and sediments of a typical estuary (Modaomen, South China): the effect of water density stratification associated with salinity. Environ. Pollut. 287, 117277 https://doi.org/10.1016/j.envpol.2021.117277.

Kouassi, N.L.B., Yao, K.M., Sangare, N., Trokourey, A., Metongo, B.S., 2019. The mobility of the trace metals copper, zinc, lead, cobalt, and nickel in tropical estuarine sediments, Ebrie Lagoon, Côte d'Ivoire. J. Soils Sediments 19, 929–944. https://doi.org/10.1007/s11368-018-2062-8.

La Colla, N.S., Negrin, V.L., Marcovecchio, J.E., Botté, S.E., 2015. Dissolved and particulate metals dynamics in a human impacted estuary from the SW Atlantic. Estuar. Coast Shelf Sci. 166, 45–55. https://doi.org/10.1016/j.ecss.2015.05.009.

Lacerda, L.D. de, Marins, R.V., Dias, F.J. da S., 2020. An arctic paradox: response of fluvial Hg inputs and bioavailability to global climate change in an extreme coastal environment. Front. Earth Sci. 8 https://doi.org/10.3389/feart.2020.00093.

Lindsey, R., 2021. Climate Change: Global Sea Level | NOAA Climate.Gov . Climate.Gov. URL. https://www.climate.gov/news-features/understanding-climate/climate-change-global-sea-level.

Liu, S., Wang, Z., Zhang, Y., Liu, Yulong, Yuan, W., Zhang, T., Liu, Yujie, Li, P., He, L., Chen, J., 2019. Distribution and partitioning of heavy metals in large anthropogenically impacted river, the Pearl River, China. Acta Geochim 38, 216–231. https://doi.org/10.1007/s11631-018-00309-7.

Luengen, A.C., Raimondi, P.T., Flegal, A.R., 2007. Contrasting biogeochemistry of six trace metals during the rise and decay of a spring phytoplankton bloom in San Francisco Bay. Limnol. Oceanogr. 52, 1112–1130. https://doi.org/10.4319/lo.2007.52.3.1112.

Ma, L., Wang, W., Xie, M.W., Wang, W.X., Evans, R.D., 2020. Using Zn isotopic signatures for source identification in a contaminated estuary of southern China. Environ. Sci. Technol. 54, 5140–5149. https://doi.org/10.1021/acs.est.9b05955.

Machado, A.A. de S., Spencer, K., Kloas, W., Toffolon, M., Zarfl, C., 2016. Metal fate and effects in estuaries: a review and conceptual model for better understanding of toxicity. Sci. Total Environ. 541, 268–281. https://doi.org/10.1016/j.scitotenv.2015.09.045.

Magalhães, F.A., Tosi, C.H., Garri, R.G., Chellappa, S., Silva, F.L., 2008. Cetacean diversity on the parnaiba delta, Maranhão state, northeastern Brazil. Braz. J. Biol. 68, 545–551. https://doi.org/10.1590/S1519-69842008000300012.

Marengo, J.A., Torres, R.R., Alves, L.M., 2017. Drought in Northeast Brazil—past, present, and future. Theor. Appl. Climatol. 129, 1189–1200. https://doi.org/10.1007/s00704-016-1840-8.

Marins, R.V., Paula Filho, F.J. De, Rodrigues Maia, S.R., De Lacerda, L.D., Marques, W.S., 2004. Distribuição de mercúrio total como indicador de poluição urbana e industrial na costa Brasileira. Quim. Nova 27, 763–770. https://doi.org/10.1590/S0100-40422004000500016.

Millero, F.J., 2013. Chemical Oceanography, fourth ed. Elsevier Oceanography Series. CRC Press, New York. https://doi.org/10.1016/S0422-9894(08)70141-7.

Mori, C., Santos, I.R., Brumsack, H., Schnetger, B., Dittmar, T., Seidel, M., 2019. Non-conservative behavior of dissolved organic matter and trace metals (Mn , Fe , Ba) driven by porewater exchange in a subtropical. Front. Mar. Sci. 6, 1–21. https://doi.org/10.3389/fmars.2019.00481.

Mosley, L.M., Liss, P.S., 2019. Particle aggregation , pH changes and metal behaviour during estuarine mixing : review and integration. Mar. Frenshwater Res. 71, 300–310. https://doi.org/10.1071/MF19195Particle.

Muehe, D., 2010. Brazilian coastal vulnerability to climate change. Pan Am. J. Aquat. Sci. 5, 1–11.

Müller, V.G., 1986. Schadstoffe in sedimenten - sedimente als schadstoffe von. Mitteilungen der Österreichischen Geol. Gesellschaft 79, 107–126. https://doi.org/10.1055/s-2007-1023171.

Nabelkova, J., Kominkova, D., 2012. Trace metals in the bed sediment of small urban streams. Open Environ. Biol. Monit. J. 5, 48–55. https://doi.org/10.2174/1875040001205010048.

Nóbrega, G.N., Ferreira, T.O., Artur, A.G., de Mendonça, E.S., Raimundo, R.A., Teixeira, A.S., Otero, X.L., 2015. Evaluation of methods for quantifying organic carbon in mangrove soils from semi-arid region. J. Soils Sediments 15, 282–291. https://doi.org/10.1007/s11368-014-1019-9.

Ollivier, P., Radakovitch, O., Hamelin, B., 2011. Major and trace element partition and fluxes in the Rhône River. Chem. Geol. 285, 15–31. https://doi.org/10.1016/j.chemgeo.2011.02.011.

Omanovic, D., Garnier, C., Oursel, B., Piz, I., 2015. Evidencing the natural and anthropogenic processes controlling trace metals dynamic in a highly stratified estuary : the Krka River estuary. Mar. Pollut. Bull. 94, 199–216. https://doi.org/10.1016/j.marpolbul.2015.02.029.

Paula Filho, F.J. de, Marins, R.V., Aguiar, J.E., Peres, T.F., Lacerda, L.D. de, 2014. Emisiones Naturales y antrópicas de Zn, Cu, Pb, Cr, Cd y Hg al Delta de Río Parnaíba/NE/Brasil. In: Marcovecchio, J.E., Botté, S.E., Freije, H. (Eds.), Procesos Geoquímicos Superficiales En Iberoamérica. Sociedad Iberoamericana de Física y Química Ambiental, Bahía Blanca, pp. 251–278.

Paula Filho, F.J. de, Marins, R.V., Lacerda, L.D. de Aguiar J.E., Peres, T.F., 2015. Background values for evaluation of heavy metal contamination in sediments in the Parnaíba River Delta estuary , NE/Brazil. Mar. Pollut. Bull. 91, 424–428. https://doi.org/10.1016/j.marpolbul.2014.08.022.

Paula Filho, F.J. de, Marins, R.V., Santos, D.V., Menezes, J.M., 2019. Accumulation of heavy metals in sediments of the Parnaíba River Delta, in: Guido, B., Lucía, S., Carolina, T., Eleonora, C. (Eds.), Actas de La V Reunión Argentina de Geoquímica de La Superficie. Asociación Argentina de Sedimentología, La Plata, pp. 138–141. http://sedici.unlp.edu.ar/handle/10915/77067.

Paula Filho, F.J. de, Marins, R.V., Santos, D.V., Pereira Junio, R.F., Menezes, J.M.C., da Gastão, F.G.C., Guzzi, A., Teixeira, R.N.P., 2021. Assessment of heavy metals in sediments of the Parnaíba River Delta in the semi-arid coast of Brazil. Environ. Earth Sci. 80, 1–17. https://doi.org/10.1007/s12665-021-09456-2.

Pavoni, E., Crosera, M., Petranich, E., Faganeli, J., Klun, K., Oliveri, P., Covelli, S., Adami, G., 2021. Distribution, mobility and fate of trace elements in an estuarine system under anthropogenic pressure: the case of the karstic timavo river (northern adriatic sea, Italy). Estuar. Coast 44, 1831–1847. https://doi.org/10.1007/s12237-021-00910-9.

Regnier, P., Wollast, R., 1993. Distribution of trace-metals in suspended matter of the scheldt estuary. Mar. Chem. 43, 3–19. https://doi.org/10.1016/0304-4203(93)90212-7.

RStudio (2022). Version 2022.12.0 + 353 "Elsbeth Geranium". RStudio: Integrated Development for R. RStudio, PBC, Boston, MA URL http://www.rstudio.com/.

Santos, T.T.L., Marins, R.V., Alves, L.P., 2023. Review on metal contamination in equatorial estuaries in the Brazilian Northeast. Front. Earth Sci. 11, 1–23. https://doi.org/10.3389/feart.2023.1142649.

Santos, T.T.L., Marins, R.V., Dias, F.J. da S., 2019. Carbon influence on metal distribution in sediment of Amazonian macrotidal estuaries of northeastern Brazil. Environ. Monit. Assess. 191, 1–16. https://doi.org/10.1007/s10661-019-7626-6.

Sedeño-Díaz, J.E., López-López, E., Mendoza-Martínez, E., Rodríguez-Romero, A.J., Morales-García, S.S., 2019. Distribution coefficient and metal pollution index in water and sediments: proposal of a new index for ecological risk assessment of metals. Water (Switzerland) 12, 1–20. https://doi.org/10.3390/w12010029.

Serejo, J.H.F., Santos, T.T.L., Lima, H.P., Azevedo, I.H.R., Dos Santos, V.H.M., Eschrique, S.A., 2020. Fortnightly variability of total suspended solids and bottom sediments in a macrotidal estuarine complex on the Brazilian northern coast. J. Sediment. Environ. 5, 101–115. https://doi.org/10.1007/s43217-020-00005-8.

Smith, F.S.G., Vital, H., Aquino da Silve, A.G., Stattegger, K., Perez, Y.A.R., 2021. Late Holoceno evolution of the Parnaíba River Delta (Brazilian Equatorial Margin): evidence of lobe switching process from mineralogical analysis and age dating on sediment cores. J. South Am. Eartg Sci. 9 https://doi.org/10.1016/j.jsames.2021.103530.

Thanh-nho, N., Strady, E., Nhu-trang, T., David, F., Marchand, C., 2018. Trace metals partitioning between particulate and dissolved phases along a tropical mangrove estuary (Can Gio , Vietnam). Chemosphere 196, 311–322. https://doi.org/10.1016/j.chemosphere.2017.12.189.

Veiga Júnior, J.P., 2000. São Luís NE/SE, Folhas SA 23-X e SA.23-Z, Estados do Maranhão e Piauí. Escala 1:500000, Programa de Levantamento Geológicos Básicos do Brasil. Companhia de Pesquisa de Recursos Minerais (CPRM), Brasília. URL. http://www.cprm.gov.br/publique/Geologia/Geologia-Basica/Projeto-Sao-Luis-NE%7CSE-556.html.

Wang, A., Wang, Z., Liu, J., Xu, N., Li, H., 2021. The Sr/Ba ratio response to salinity in clastic sediments of the Yangtze River Delta. Chem. Geol. 559, 119923 https://doi.org/10.1016/j.chemgeo.2020.119923.

Wang, W., Chen, M., Guo, L., Wang, W.X., 2017. Size partitioning and mixing behavior of trace metals and dissolved organic matter in a South China estuary. Sci. Total Environ. 603–604, 434–444. https://doi.org/10.1016/j.scitotenv.2017.06.121.

Wang, W., Wang, W.X., 2016. Phase partitioning of trace metals in a contaminated estuary influenced by industrial effluent discharge. Environ. Pollut. 214, 35–44. https://doi.org/10.1016/j.envpol.2016.03.059.

Wu, F., Harper, B.J., Harper, S.L., 2019. Comparative dissolution, uptake, and toxicity of zinc oxide particles in individual aquatic species and mixed populations. Environ. Toxicol. Chem. 38, 591–602. https://doi.org/10.1002/etc.4349.

Yao, Q., Wang, X., Jian, H., Chen, H., Yu, Z., 2016. Behavior of suspended particles in the Changjiang Estuary: size distribution and trace metal contamination. Mar. Pollut. Bull. 103, 159–167. https://doi.org/10.1016/j.marpolbul.2015.12.026.